Science Advances
AAAS

advances.sciencemag.org/cgi/content/full/6/38/eabc5529/DC1

Supplementary Materials for

Expanding and optimizing 3D bioprinting capabilities using complementary network bioinks

Liliang Ouyang, James P. K. Armstrong, Yiyang Lin, Jonathan P. Wojciechowski, Charlotte Lee-Reeves, Daniel Hachim, Kun Zhou, Jason A. Burdick, Molly M. Stevens*

*Corresponding author. Email: m.stevens@imperial.ac.uk

Published 18 September 2020, *Sci. Adv.* **6**, eabc5529 (2020)
DOI: 10.1126/sciadv.abc5529

This PDF file includes:

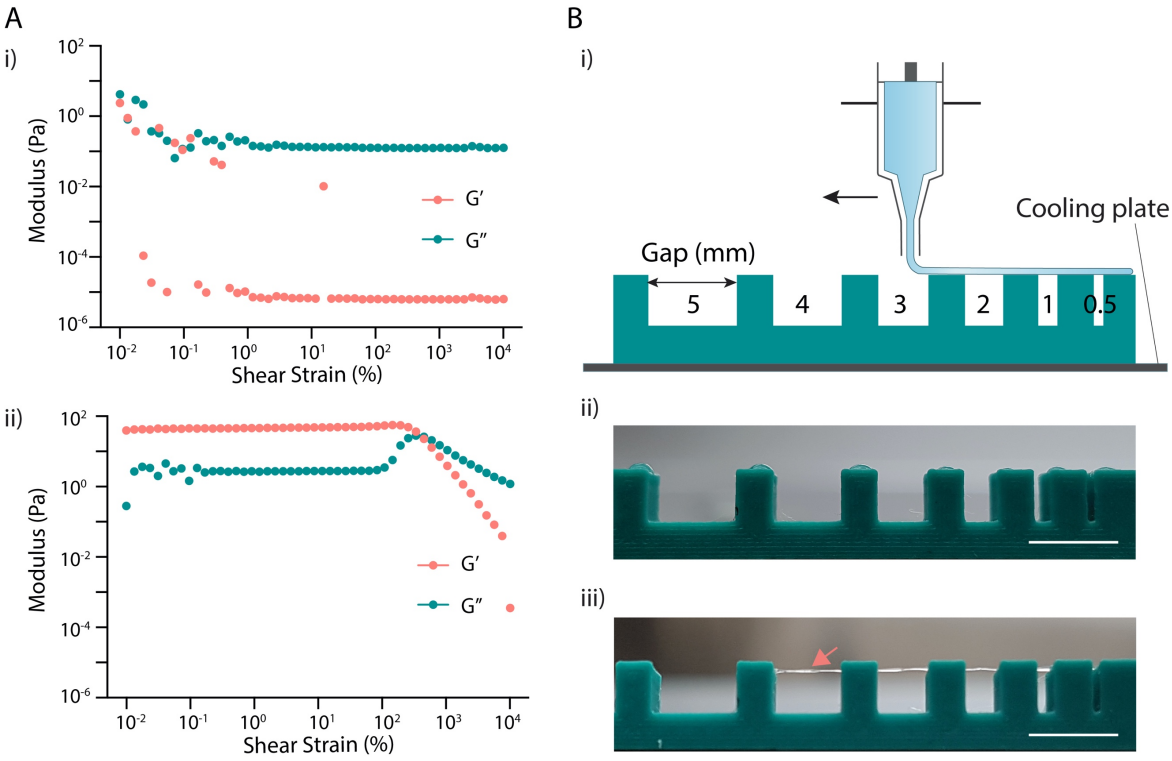

Figure S1. Printability characterization. (**A**) Oscillatory strain sweeps (frequency of 1.5 Hz, temperature of 25 °C) showing typical shear-thinning behavior of (i) 2.5 wt% $HAMA^+$, while (ii) HAMA without gelatin was in a liquid phase across the tested strain range. (**B**) (i) Experimental setup of self-supporting bioink filament formation. Representative optical images for (ii) 2.5 wt% HAMA and (iii) 2.5 wt% $HAMA^+$ bioinks (arrow indicates filament formation). HAMA failed to bridge the smallest gap (0.5 mm), while $HAMA^+$ filaments could be used to bridge gaps of up to 4 mm. Printing parameters can be found in Table S1 corresponding to individual bioink. Scale bars: 5 mm. Credit for all photographs in this figure: Liliang Ouyang, Imperial College London.

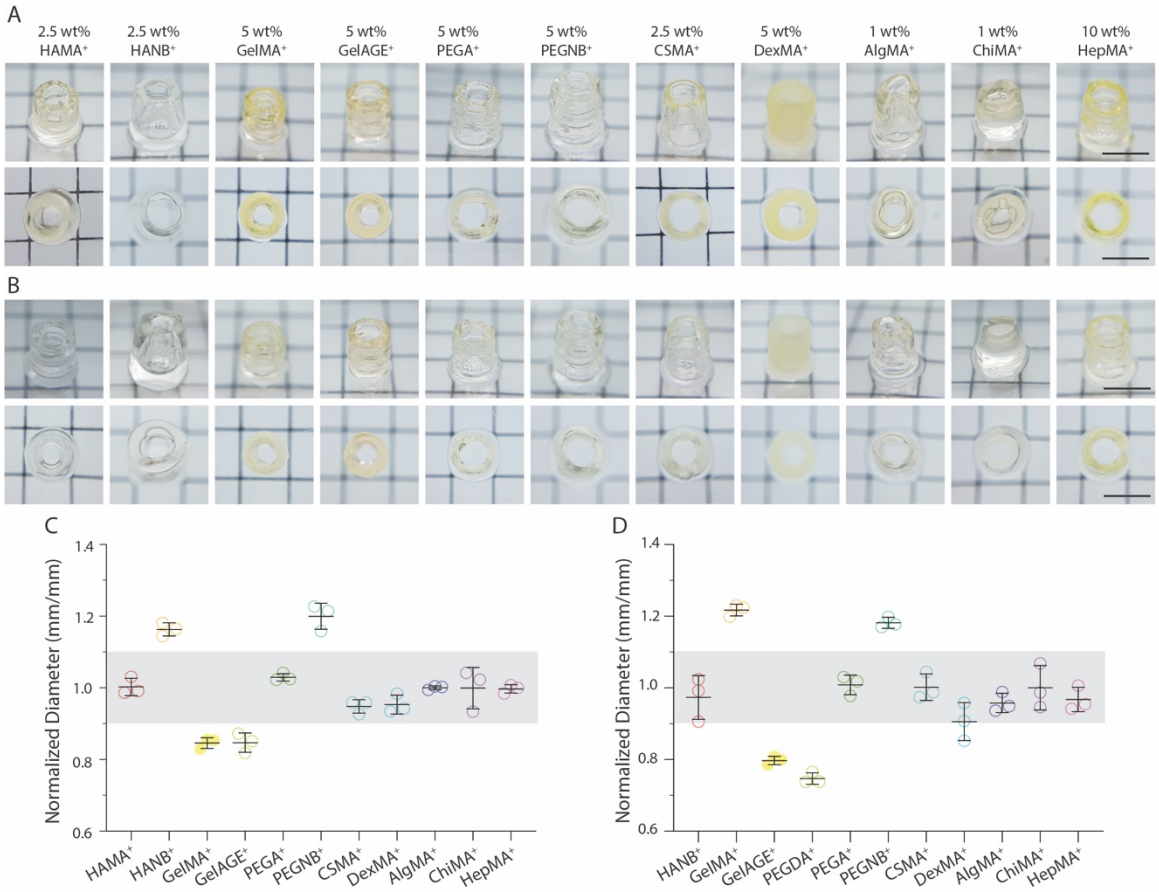

Fig. S2. Stability of printed constructs. (A–B) Images of printed tubes and **(C–D)** corresponding diameter changes 1 d (A, C) and 7 d (B, D) after printing and during incubation at 37 °C (normalized to the values at 0 d). Scale bars: 5 mm. Credit for all photographs in this figure: Liliang Ouyang, Imperial College London.

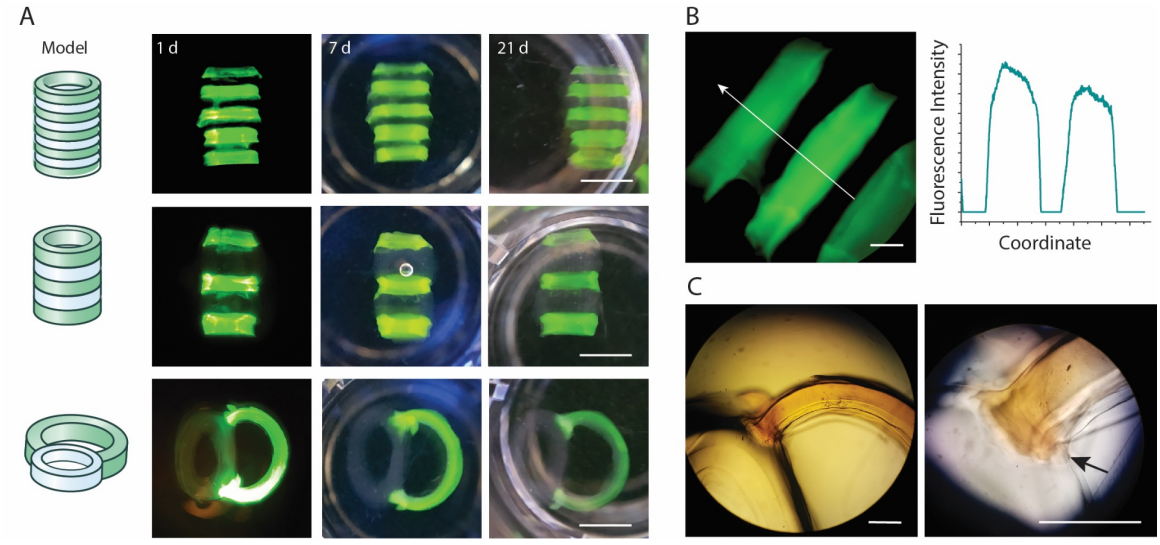

Fig. S3. Structural heterogeneity. (A) Photographs of printed heterogeneous constructs (tubular and tracheal-esophageal model) after (1 d, 7 d, 21 d) incubation at 37 °C. 2.5 wt%

HAMA$^+$ (clear phase) and 5 wt% GelMA$^+$ (green phase) were printed alternately along the longitudinal or transverse direction. **(B)** Microscopy image of the heterogeneous tube and fluorescence intensity profile along the indicated white line. **(C)** Microscopy images of a tracheal-esophageal construct, indicating the interface between two phases (arrow). Scale bars: 5 mm (A), 1 mm (B–C). Credit for all photographs in this figure: Liliang Ouyang, Imperial College London.

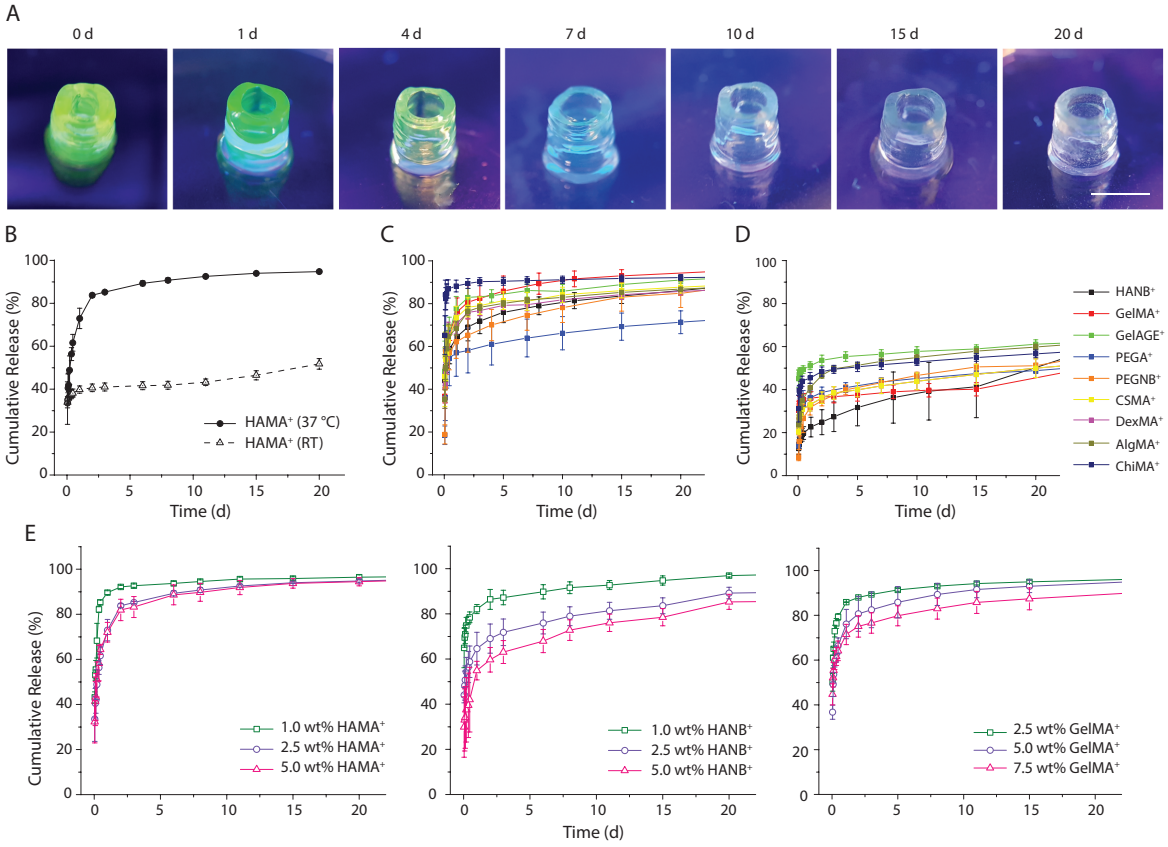

Fig. S4. Release of gelatin. (A) Representative images of a 3D printed tubular structure (2.5 wt% HAMA$^+$) over time during incubation at 37 ℃. The green fluorescence indicates the embedded Fluorescein-gelatin. **(B)** Accumulated release of gelatin from 2.5 wt% HAMA$^+$ hydrogels during incubation at 37 ℃ or room temperature (RT). Gelatin release profiles in various complementary network hydrogels incubated at **(C)** 37 ℃ and **(D)** room temperature. **(E)** The influence of photo-crosslinkable polymer concentration (HAMA$^+$, HANB$^+$, GelMA$^+$) on gelatin release. Scale bar: 5 mm. Credit for all photographs in this figure: Liliang Ouyang, Imperial College London.

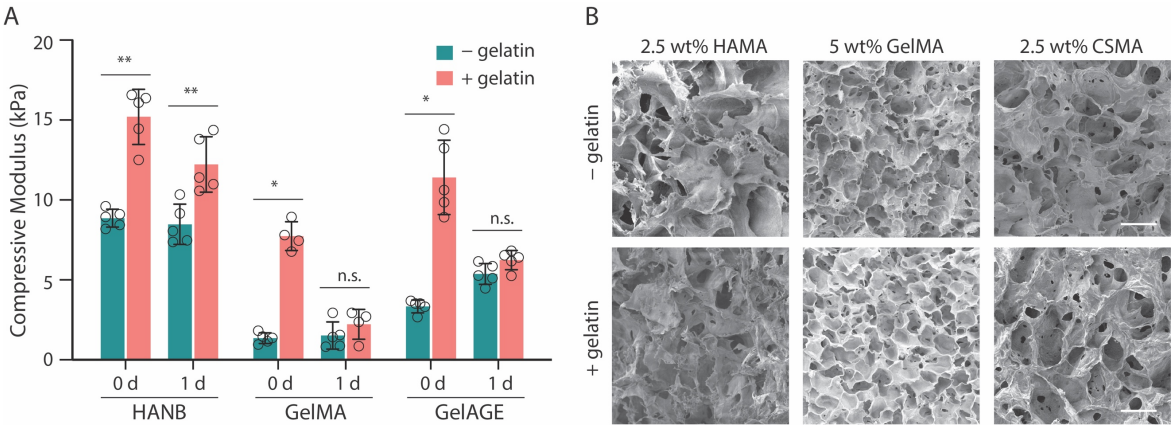

Fig. S5. Influence of gelatin on mechanical properties and microstructure. **(A)** The compressive modulus of HANB, GelMA, and GelAGE hydrogels with or without supplementary 5 wt% gelatin. 0 d and 1 d indicate the conditions before and after 24 h incubation at 37 °C, respectively. Two-tailed Mann–Whitney test, *$p < 0.05$, n.s. = not significant ($n \geq 3$). **(B)** Representative scanning electron micrographs of various hydrogels with or without supplementary 5 wt% gelatin. Hydrogels were analyzed after 24 h incubation followed by freeze-drying. Scale bars: 100 µm.

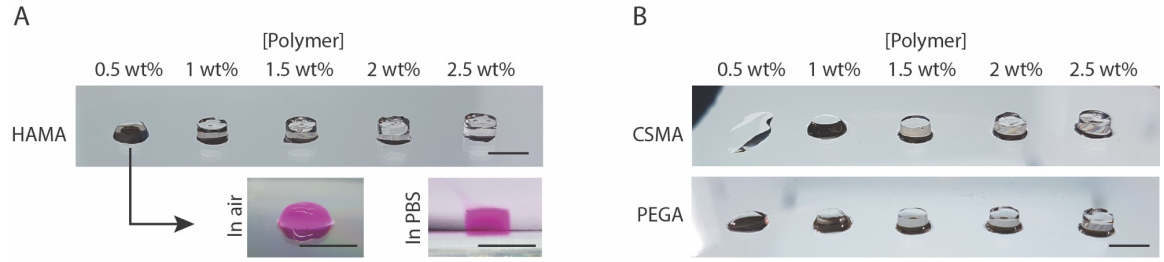

Fig. S6. Concentration screening for hydrogel formation. Images of cast cylinder hydrogels (diameter 3.5 mm, height 2 mm) for **(A)** HAMA, **(B)** CSMA and PEGA with varied polymer concentrations. All samples were treated with light (365 nm, 10 mW cm^{-2}) for 5 min before demolding. Cylindrical 0.5 wt% HAMA hydrogels were stained with dye (magenta) to visualize their geometry in air and PBS. Scale bars: 5 mm. Credit for all photographs in this figure: Liliang Ouyang, Imperial College London.

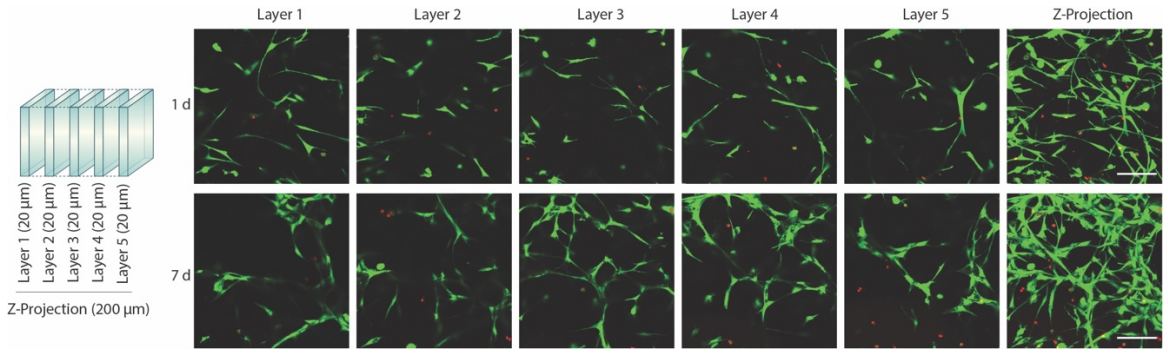

Fig. S7. Uniformity of cell distribution. Confocal microscopy z-stack images (green for calcein-AM, red for ethidium homodimer-1) of astrocytes encapsulated in bioprinted constructs at different depths within the hydrogel. Scale bars: 100 µm.

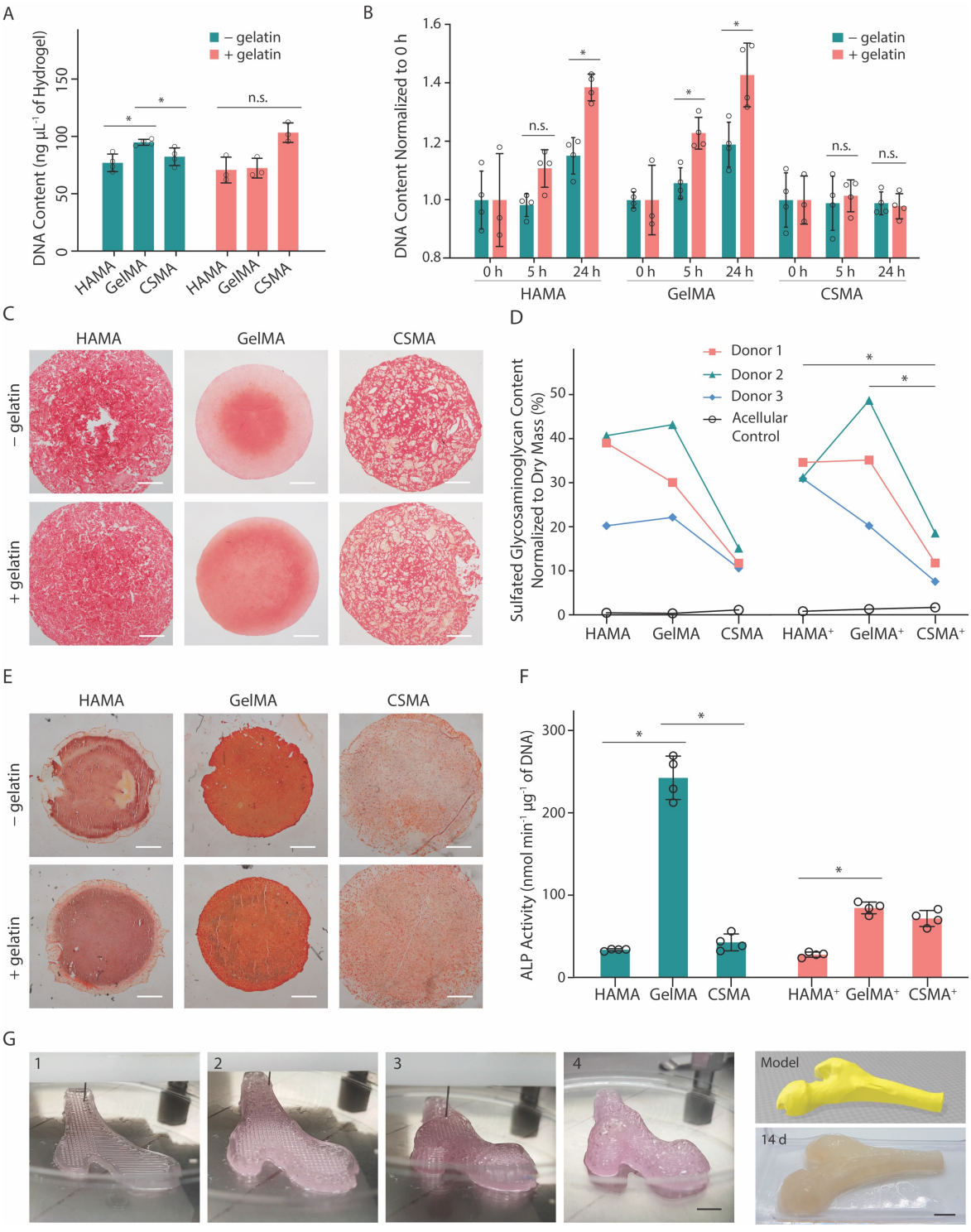

Fig. S8. Comparison of tissue formation. **(A)** DNA quantity at 0 h and **(B)** fold change in DNA quantity (normalized to 0 h) of Saos-2 laden hydrogels determined by a PicoGreen™ assay. Two-tailed Mann–Whitney test, *$p < 0.05$, n.s. = not significant ($n \geq 3$). **(C)** Safranin O staining of cartilage-like construct engineered using chondrocytes encapsulated (2.5 ×

10^7 mL^{-1}) in hydrogels with or without supplementary 5 wt% gelatin after culturing for 42 d. **(D)** The fraction of sulfated glycosaminoglycan (normalized to total dry tissue mass) in cartilage engineered from chondrocyte-laden hydrogels. Tissue constructs were harvested at 42 d and digested, before measuring sulfated glycosaminoglycan content using a DMMB assay. Paired Wilcoxon test, *$p < 0.05$ (donor number = 3). **(E)** Alizarin Red S staining and **(F)** normalized ALP activity of bone-like construct engineered using Saos-2 cells encapsulated in the same set of hydrogels (initial cell density of 7.5×10^6 mL^{-1}). Analysis was performed after culturing the cellularized hydrogels for 14 d. Two-tailed Mann–Whitney test, *$p < 0.05$. **(G)** Bioprinting of a centimeter-sized bone-shaped construct using 5 wt% $GelMA^+$ bioink encapsulated with Saos-2 cells. Numbers (1-4) on the images indicate the printing process. Scale bars: 500 μm (C, E), 5 mm (G). Credit for all photographs in this figure: Liliang Ouyang, Imperial College London.

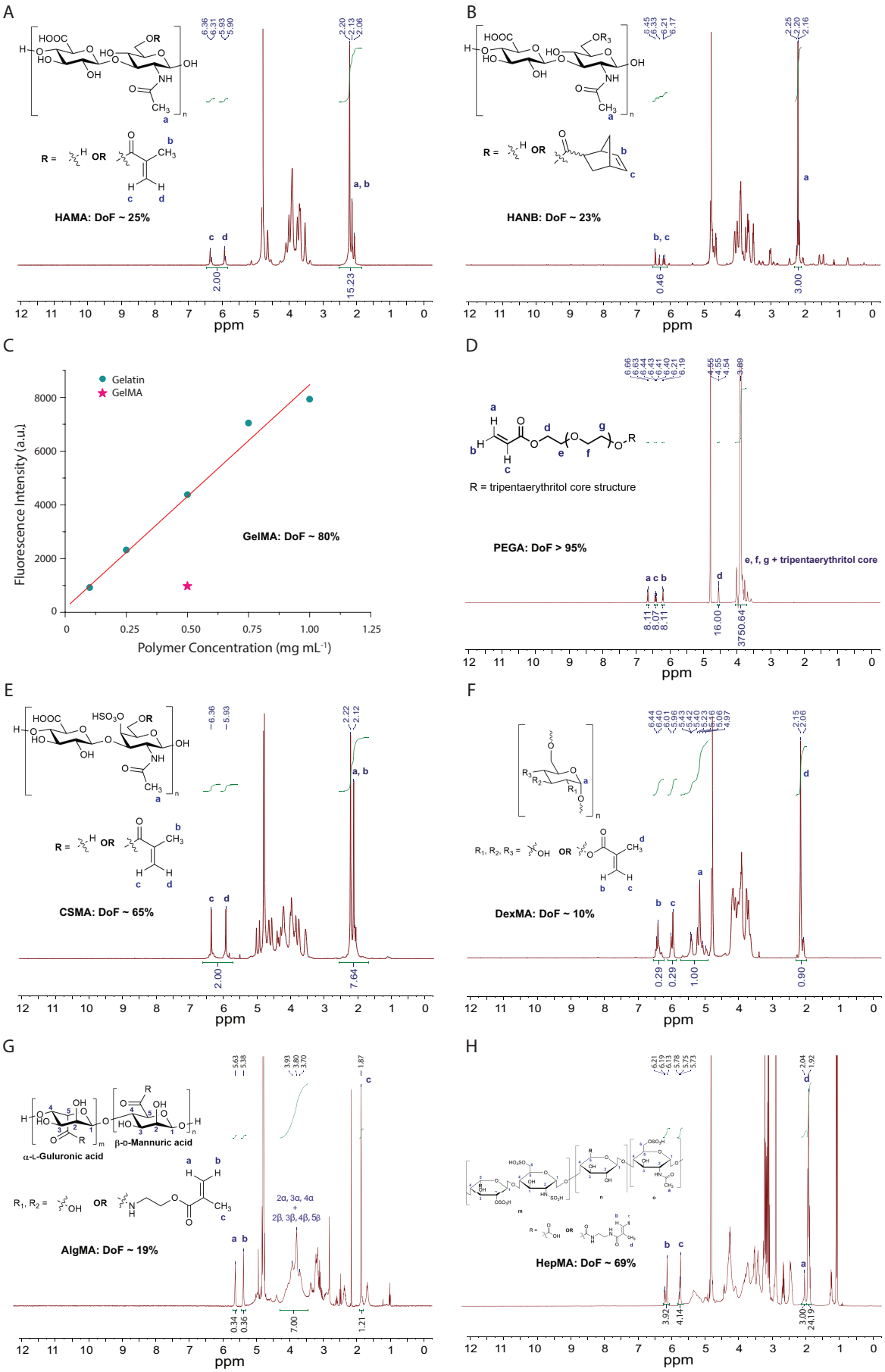
A
HAMA: DoF ~ 25%
B
HANB: DoF ~ 23%
C
Gelatin
GelMA
Fluorescence Intensity (a.u.)
Polymer Concentration (mg mL-1)
GelMA: DoF ~ 80%
D
R = tripentaerythritol core structure
PEGA: DoF > 95%
e, f, g + tripentaerythritol core
E
CSMA: DoF ~ 65%
F
DexMA: DoF ~ 10%
G
α-L-Guluronic acid
β-D-Mannuric acid
AlgMA: DoF ~ 19%
H
HepMA: DoF ~ 69%
ppm

Fig. S9. Determination of degree of functionalization. ^{1}H-NMR spectrum for **(A)** HAMA, **(B)** HANB, **(D)** PEGA, **(E)** CSMA, **(F)** DexMA, **(G)** AlgMA, **(H)** HepMA and **(C)** Fluoraldehyde^{TM} assay data of GelMA.

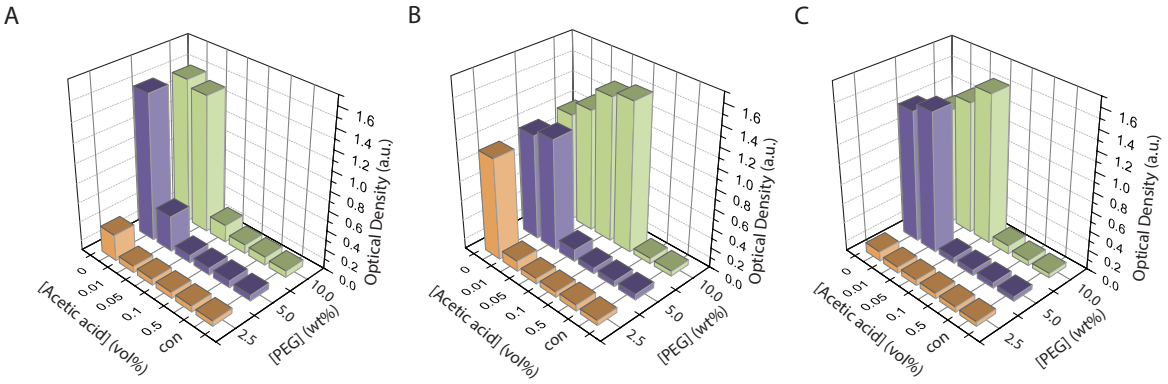

Fig. S10. Solvent optimization for PEG-based bioinks. The optical density of **(A)** PEGDA, **(B)** PEGA, and **(C)** PEGNB containing different concentrations of acetic acid (from 0 to 0.5 vol%) and PEG (from 2.5 to 10 wt%). The control (con) indicates a condition free of gelatin and acetic acid. All other conditions are presented with 5 wt% gelatin.

Table S1. Bioink composition and examples of printing parameters.

Bioink Name	Bioink Composition				Printing Parameters			
	[Base Polymer] (wt%)	[Gelatin] (wt%)	[LAP] (mM)	[DTT] (mM)	Nozzle Temp. (°C)	Platform Temp. (°C)	Pneumatic Pressure (bar)	Printing Speed (mm s^{-1})
2.5 wt% HAMA	2.5	-	2	-	25-26	15	0.1-0.2	2-3
2.5 wt% HAMA^{+}	2.5	5	2	-	25-26	15	0.8-1.1	2-3
0.5 wt% HAMA^{+}	0.5	5	2	-	24-25	15	0.4-0.6	2
1 wt% HAMA^{+}	1.0	5	2	-	~25	15	0.7-0.9	2
5 wt% HAMA^{+}	5.0	5	2	-	25-26	15	0.7-0.9	2
10 wt% HAMA^{+}	10.0	5	2	-	26-27	15	1.6-1.9	2
2.5 wt% GelMA^{+}	2.5	5	2	-	24-25	15	0.5-0.6	1.5-2
5 wt% GelMA^{+}	5.0	5	2	-	26-27	15	0.5-0.7	1.5-2.5
5 wt% GelAGE^{+}	5.0	5	2	3	26-27	15	0.6-0.8	2
2.5 wt% HANB^{+}	2.5	5	2	2.31	23-24	15	0.6-0.7	1.5-2.5
5 wt% PEGDA^{+}	5.0	5	2	-	26-27	15	0.8-1.0	2-3
1.5 wt% PEGA^{+}	1.5	5	2	-	25-26	15	0.5-0.7	2-3

2.5 wt% PEGA[+]	2.5	5	2	-	25-26	15	0.6-0.8	2-3
5 wt% PEGA[+]	5.0	5	2	-	26-27	15	0.7-0.8	2-3
5 wt% PEGNB[+]	5.0	5	2	4	24-25	15	0.8-0.9	2-3
5 wt% DexMA[+]	5.0	5	2	-	24-25	15	0.6-0.7	2-3
1.5 wt% CSMA[+]	1.5	5	2	-	~25	15	0.4-0.6	2
2.5 wt% CSMA[+]	2.5	5	2	-	24-25	15	0.7-0.8	2-3
1 wt% AlgMA[+]	1.0	5	2	-	25-26	15	0.7-0.8	2
1 wt% ChiMA[+]	1.0	5	2	-	25-26	15	0.6-0.9	2
10 wt% HepMA[+]	10.0	5	2	-	24-25	15	0.8-0.9	2